Refractivity virial coefficients of gaseous CH4, C2H4, C2H6, CO2, SF6, H2, N2, He, and Ar

H. J. Achtermann, G. Magnus, and T. K. Bose

Citation: J. Chem. Phys. **94**, 5669 (1991); doi: 10.1063/1.460478
View online: http://dx.doi.org/10.1063/1.460478
View Table of Contents: http://jcp.aip.org/resource/1/JCPSA6/v94/i8
Published by the AIP Publishing LLC.

Refractivity virial coefficients of gaseous CH_4, C_2H_4, C_2H_6, CO_2, SF_6, H_2, N_2, He, and Ar

H. J. Achtermann and G. Magnus
Institut für Thermodynamik, Universität Hannover, D-3000 Hannover, Germany

T. K. Bose
Départment de Physique, Group de recherche sur les diélectriques, Université sité de Québec à Trois-Rivières, C. P 500 Trois-Rivières, Québec, Canada G9A 5H7

(Received 23 May 1990; accepted 7 January 1991)

Accurate values of the second and third refractivity virial coefficients B_R and C_R of gaseous CH_4, C_2H_4, C_2H_6, CO_2, SF_6, H_2, N_2, He (only B_R is given), and Ar have been measured using the recently improved differential-interferometric technique. This device basically consists of two coupled grating interferometers. During the overflow experiment of the gas one interferometer, with two similar cells in series, measures differentially the higher-order effects of density, and the second interferometer, with two similar cells in parallel, measures at the same time the absolute value of the refractive index. The second interferometer is also used for an accurate control of the decompression during the overflow experiment. It is thus possible to extend the overflow experiments to high values of pressure. The overflow experiments were carried out up to pressures of 35 MPa. The density range extends up to two times the critical density. The third refractivity virial coefficient C_R becomes significant for all the gases examined, except for He, when the measurements approach approximately the value 0.3 of the reduced density ρ/ρ_c. The fourth refractivity virial coefficient D_R becomes significant for C_2H_4, C_2H_6, and SF_6 when ρ/ρ_c approach approximately the value of one. The agreement between the classically calculated values of B_R, based on the dipole induced dipole model, and our experimental B_R values is very good for CH_4, C_2H_4, C_2H_6, SF_6, and Ar, but poor for CO_2, H_2, N_2, and He. For He however, the quantum mechanical calculation of B_R obtained by including both the long-range and the short-range effects on the polarizability is in remarkably good agreement with our experimental B_R value. Accurate values of the first refractivity virial coefficients A_R were determined independently by making absolute measurements of the refractive index as a function of pressure.

I. INTRODUCTION

The purpose of this paper is to investigate the density dependence of the refractivity of gases. It is convenient to use the virial expansion of the refractivity of gases, R_m, as a power series in ρ, the density in moles per unit volume[1,2]

$$R_m = (n^2-1)/(n^2+2)\rho = A_R + B_R\rho + C_R\rho^2 + D_R\rho^3 + \cdots, \quad (1)$$

where A_R, B_R, C_R, D_R,... are, respectively, the first, second, third, fourth,... refractivity virial coefficients, which are independent of ρ, but are functions of frequency[3-7] and temperature.[8]

The first refractivity virial coefficient A_R describes the isolated molecule contribution to R_m. The second refractivity virial coefficient B_R describes the excess contribution to R_m due to the interactions of molecular pairs, and in the past two decades it has been the subject of many experimental[6-19] and theoretical[1,6,13-15,20] investigations. The third refractivity virial coefficient C_R describes the interaction of molecular triplets. Only very approximate theoretical calculations exist for C_R.[20] The physical meaning of the refractivity virial coefficients beyond the third is not available; they are merely fitting parameters. In order to obtain B_R accurately we need to determine at least the contribution of the C_R term. As a general rule, the accuracy of the second or a higher-order refractivity virial coefficient improves if the measurements are carried out in the region of pressure or refractive index where the contribution of the succeeding virial term is significant.

The independent method of determining A_R, the zero density limit, is based on isothermal measurements of the refractive index as a function of pressure.[19]

For the determination of B_R, C_R,..., one finds two methods in the literature: the absolute method and the differential method.

The absolute method is based on combining measurements of the refractive index $n(P,T)$ with density data $\rho(P,T)$.[7-11] In this method the accuracy of the calculated R_m values is limited by the accuracy of the $\rho(P,T)$ data, since the refractive index is known much more precisely than the density.[8,9]

The differential method is based on measuring directly the effects of molecular interactions on the refractivity of gases. This new differential-interferometric technique is proposed by Buckingham *et al.*,[2] and first used by Buckingham and Graham[12] and St-Arnaud and Bose.[13] The method consists in measuring differentially the total optical path when a gas is decompressed from one cell into a similar evacuated cell. This technique became even more important with the recent development of the independent optical method for the precise determination of *PVT* values from refractive in-

 0021-9606/91/085669-16$03.00

dex measurements,[16-19] because an accurate knowledge of the refractivity virial coefficients offers a potentially useful method of density gauging through refractive index measurements. To obtain precise values of B_R, C_R,..., the overflow experiments must be carried out up to the highest pressures practicable.[18,19]

The direct measurement of the excess contribution to R_m in relatively high pressure region (30 MPa) is very difficult and time consuming, because refractivity virial effects are very small and as such unsuitable for a satisfactory adjustment of the allowable flowrate in the expansion valve during the overflow procedure. If the allowable flowrate is exceeded by a small amount, this leads to a collapse of the interference fringe count.

To overcome these difficulties, Achtermann and Baehr[18] have improved the differential-interferometric technique by developing a device consisting of two coupled grating interferometers. One interferometer, with two similar cells in series, measures differentially the excess contribution to R_m and the second interferometer, with two similar cells in parallel, measures at the same time the absolute value of the refractive index. The measured independent variable in the second interferometer is about a hundredfold of the measured dependent variable in the interferometer with two cells in series. The second interferometer is therefore also used for an accurate control of the decompression in the two interferometers during the overflow experiment and to adjust the optimal flowrate during the expansion procedure. It is thus possible to extend the overflow experiments to high values of pressure. The new device was used for the direct measurement of the excess contribution to R_m up to pressures of 35 MPa.

In this paper we give our experimental results of B_R and C_R for CH_4, C_2H_4, C_2H_6, CO_2, SF_6, H_2, N_2, He (only B_R is given), and Ar. A novel feature of the measurements on C_2H_4, C_2H_6, and SF_6 is the significant contribution of the fourth term $D_R\rho^3$, Eq. (1), in the investigated range of pressure. Separate measurements of the refractive index as a function of pressure were made in the range 0.1–35 MPa, and accurate values of the first refractivity virial coefficient A_R were determined from this. A rough estimate of the accuracy of the measured first refractivity virial coefficient is A_R, $\pm 0.02\%$ and the accuracy of the higher-order coefficients, except for H_2 and He, is B_R, $\pm$ 2–5%; C_R, $\pm$ 3–5%; and D_R, $\pm$ 30–50%. Comparisons of our results with the existing experimental and theoretical refractivity virial coefficients from the literature are also presented.

II. EXPERIMENT

The independent determination of B_R, C_R, D_R,... is based on the measurement of the excess contribution of the function $(n-1)\rho^{-1}$, which is directly related to the refractive index virial coefficients B_n, C_n, D_n,..., defined by

$$(n-1)\rho^{-1} = A_n + B_n\rho + C_n\rho^2 + D_n\rho^3 + \cdots. \quad (2)$$

If one compares the coefficients of ρ^i in Eq. (2) with those in Eq. (1) it is readily shown that

$$A_R = 2A_n/3, \quad (3)$$

$$B_R = 2B_n/3 - A_n^2/9, \quad (4)$$

$$C_R = 2C_n/3 - 2A_nB_n/9 - 4A_n^3/27, \quad (5)$$

$$D_R = 2D_n/3 - 2A_nC_n/9 - B_n^2/9 - 4A_n^2B_n/9 + 11A_n^4/81. \quad (6)$$

The direct determination of B_n, C_n, D_n,... consists of measuring the change of the sum of optical path lengths of two identical sample cells during an overflow experiment. Initially, one cell is filled with the gaseous sample at density ρ_1 and the other is evacuated. Then, by opening the expansion valve between the two cells, the sample is shared with the previously evacuated cell, and at the end of the expansion procedure the initial density ρ_1 is halved. Due to the halving of the density ($\rho_2 = \rho_1/2$) and the doubling of the length of the cell filled with the sample ($l_2 = 2l_1$), the linear term in density ($lA_n\rho$) remains the same before and after the overflow experiment. If $(n-1)$ were proportional to the density, the change of optical path lengths given by Eq. (7) would be zero, but departures from proportionality arising from molecular interactions and bulk polarization effects produce a change of the optical path lengths that is directly related to B_n, C_n, D_n,... .

For perfectly matched cells we thus obtain

$$\begin{aligned}\lambda_0(K_1 - K_2) &= l[(n_1 - 1) - 2(n_2 - 1)] \\ &= l[(1/2)B_n\rho_1^2 + (3/4)C_n\rho_1^3 + (7/8)D_n\rho_1^4 + \cdots],\end{aligned} \quad (7)$$

where n_1 and n_2 are the initial and final values of the refractive index, $\lambda_0 K_1$ and $\lambda_0 K_2$ are the initial and final values of the measured change of the optical path lengths referred to vacuum, λ_0 is the vacuum wavelength of the laser light, and l is the length of each cell. Because the density dependence of $(n-1)\rho^{-1}$ is very small, the number of fringes K_1 and K_2 are nearly equal. To reduce the errors resulting from taking the difference between two numbers of nearly equal magnitude, K_1 and K_2, it is much more accurate to measure directly the change of the optical path lengths during the actual expansion procedure by counting the change $\Delta K = (K_1 - K_2)$ of the interference fringes instead of measuring K_1 during the filling procedure and K_2 after the expansion procedure while venting the sample to vacuum. Nevertheless, one still has to measure K_1, the independent variable of $\Delta K = \Delta K(K,T)$.

In practice, it is not possible to construct identical cells. The unavoidable mismatch in cell lengths and volumes lead to systematic errors in the fringe count ΔK. These mismatch effects are eliminated by carrying out two successive expansions in opposite directions.[6,12-19]

Using the expansion technique, the expansion from cell A to cell B gives the relation $\Delta K_{AB}(K_A,T)$. The initial state of cell A filled with the sample gas is determined by the variable $K_A(T)$. Similarly, if cell B contains gas and cell A is evacuated, the expansion from cell B to cell A gives the relation $\Delta K_{BA}(K_B,T)$.

On adding the two relations, the systematic errors due to the mismatch in cell lengths and volumes in ΔK_{AB} and ΔK_{BA} are canceled. One then obtains the relation between

the measured variables and the refractive index virial coefficients B_n, C_n, D_n,..., given by

$$F = \Delta K_{AB}/K_A + \Delta K_{BA}/K_B$$
$$= B_n(2A_n^2)^{-1}[(n_A-1)+(n_B-1)] + (3A_nC_n - 4B_n^2)(4A_n^4)^{-1}[(n_A-1)^2+(n_B-1)^2]$$
$$+ (20B_n^3 - 26A_nB_nC_n + 7A_n^2D_n)(8A_n^6)^{-1}[(n_A-1)^3+(n_B-1)^3] + \cdots, \quad (8)$$

where for convenience the symbol F is used for the so-called refractive index function, and where $n_A - 1 = K_A\lambda_0/l$ and $n_B - 1 = K_B\lambda_0/l$.

The measurements are carried out in such a way that K_A is nearly equal to K_B. This increases the efficiency of the error compensation, because the systematic errors in ΔK_{AB} and ΔK_{BA} approach each other when K_A is equal to K_B. The variable in the second term of Eq. (8) can then be written as $(n_A-1)^2+(n_B-1)^2 \simeq [(n_A-1)+(n_B-1)]^2/2$ and in the third term as $(n_A-1)^3+(n_B-1)^3 \simeq [(n_A-1)+(n_B-1)]^3/4$. Making a least-squares fit of Eq. (8) to a polynomial in $[(n_A-1)+(n_B-1)]$, one can determine B_n from the slope and the significant succeeding coefficients C_n, D_n, ... from the curvature.

The experimental apparatus previously described in detail, essentially consists of two coupled grating interferometers.[18,19] Both the differential measurements of $\Delta K(K,T)$ to determine B_R, C_R, D_R,... and the separate measurements of the refractive index $n(P,T)$ to determine A_R have been carried out with the same interferometer system, Fig. 1.

The differential measurements to obtain ΔK take place in interferometer I with the two cells 1 and 3 in series. Interferometer II is used to measure K, the independent variable of ΔK, which determines the initial state of the overflow experiment. To provide the total fringe count K, the two cells 2 and 4 of interferometer II are in parallel. The correlated cells are connected with each other, Fig. 1. The coupled interferometers make it possible to obtain ΔK and K simultaneously during the overflow experiment.

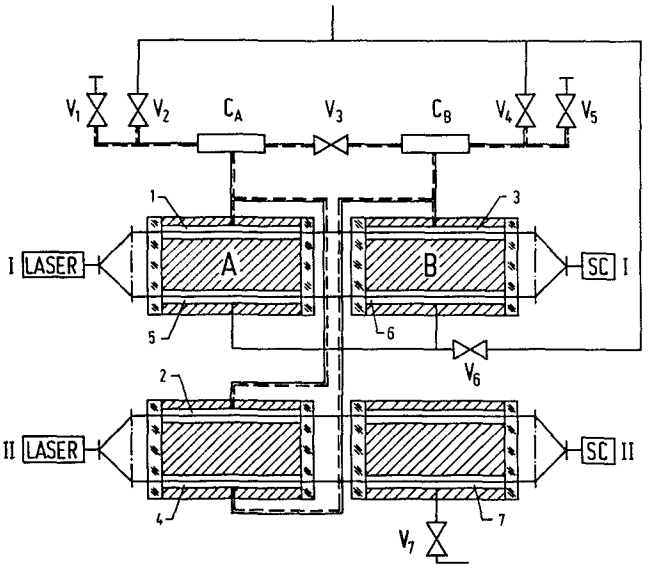

FIG. 1. Schematic drawing of the two coupled interferometers I and II for isothermal differential measurements of the refractive index function F and of the refractive index $n(P,T)$. Cells 1, 2, 3, and 4 are used for the measurements of F, and cells 5, 6, and 7 for the $n(P,T)$ measurements. V_1 to V_7 represent different valves, C_A and C_B two compensating chambers, and SC I and SC II two signal converters (optic–electric).

Each cell system (A and B) contains a compensation chamber (C_A and C_B) which facilitates the controlled overflow experiment because the volume of each cell, less than 1 cm^3, is very small. The volume of each compensation chamber is approximately 100 cm^3. The cell systems were matched by means of two valves (V_1 and V_5) by fractionally advancing or withdrawing the stems of the open valves in order to obtain nearly identical volumes. The optical procedure for this, in which CH_4 with the well-known values of B_R and C_R is used as a reference gas, has recently been described.[18] The matching of the cell systems is preferable, because the noncompensated systematic error of higher orders is then negligible.

In the following we consider the expansion procedure from the cell system A with the cells 1 and 2 to the cell system B with the cells 3 and 4.

The changes of the index of refraction during the overflow process are identical in the expansion cells 1 and 2, as well as in the compression cells 3 and 4. The change of the fringe count in the individual cells 1 and 2 is given by

$$\Delta K_1 = \Delta K_2 = l\lambda_0^{-1}[(n_1-1)-(n_2-1)]$$
$$= l\lambda_0^{-1}[(1/2)A_n\rho_1 + (3/4)B_n\rho_1^2 + (7/8)C_n\rho_1^3 + \cdots], \quad (9)$$

and, equivalently, in the initially evacuated cells 3 and 4 with $n_1 = 1$

$$\Delta K_3 = \Delta K_4 = l\lambda_0^{-1}[-(n_2-1)]$$
$$= l\lambda_0^{-1}[-((1/2)A_n\rho_1 + (1/4)B_n\rho_1^2 + (1/8)C_n\rho_1^3 + \cdots)]. \quad (10)$$

In interferometer I the changes of the index of refraction take place in the same beam. In this case we obtain the resultant change of the fringe count $\Delta K_{AB,I}$ by adding the individual values of ΔK_1 and ΔK_3

$$\Delta K_{AB,I} = \Delta K_1 + \Delta K_3$$
$$= l\lambda_0^{-1}[(1/2)B_n\rho_1^2 + (3/4)C_n\rho_1^3 + \cdots]. \quad (11)$$

Due to the partial compensation between ΔK_1 and ΔK_3, the resultant change of the fringe count $\Delta K_{AB,I}$ is only related to terms with the higher-order refractive index virial coefficients B_n, C_n, ...

In interferometer II the changes of the index of refrac-

tion take place in the two different beams (see Fig. 1), thereby avoiding the effect of compensation. In this case we obtain the resultant change of the fringe count $\Delta K_{AB,II}$ on subtraction of the individual values of ΔK_2 and ΔK_4

$$\Delta K_{AB,II} = \Delta K_2 - \Delta K_4 = l\lambda_0^{-1}(A_n\rho_1 + B_n\rho_1^2 + C_n\rho_1^3 + \cdots) = K_1 = K. \quad (12)$$

Due to the lack of compensation between ΔK_2 and ΔK_4, the cumulative changes of fringes in interferometer II, $\Delta K_{AB,II}$, is not only related to terms with the higher-order refractive index virial coefficients B_n, C_n,..., but also to the linear term with the first refractive index virial coefficient A_n. The value of $\Delta K_{AB,II}$ is thus equal to an absolute refractive index measurement, which corresponds to a change of density between zero (initially evacuated cell) and the density ρ_1 (initially filled cell). The integrated fringe count is equal to an absolute fringe count K, the independent variable of the differentially measured value of ΔK.

The fringe count K is about a hundredfold of the fringe count ΔK. Interferometer II therefore acts as a guiding instrument for the accurate control of decompression during the overflow experiment. The changes of fringes are indicated by the rotating electric fields, produced from the optical signals of the grating interferometers. The flowrate of the expansion valve (V_3) placed between C_A and C_B is indicated exactly by the sensitive rotating electric field of interferometer II which is about 100 times faster than that of interferometer I.

It is worth noting that interferometer II is mainly designed for adjusting the maximum flowrate in the expansion valve in order to optimize the direct fringe count of ΔK and to make direct differential measurements of ΔK possible in high pressure regions.

The measurement of the refractive index and the pressure, $n(P,T)$, to determine A_R is carried out by using the same two interferometers I and II as for the $\Delta K(K,T)$ measurements. For the determination of the refractive index of the sample, we use interferometer I with the cells 5 and 6, Fig. 1. Interferometer II with the cell 7 is used to determine the pressure by measuring the refractive index of nitrogen at a fixed temperature. The relation between the refractive index of nitrogen and the pressure has been previously established by using a precision piston gauge.[21] The coupled interferometers make it possible to obtain the refractive index and the pressure simultaneously during the expansion run. The apparatus and the procedure for the absolute measurement of the refractive index as a function of pressure have recently been described.[16–19]

III. RESULTS

Determination of the first- and the higher-order refractivity virial coefficients have been made for nine gases, namely, CH_4, C_2H_4, C_2H_6, CO_2, SF_6, H_2, N_2, He, and Ar. The measurements were carried out with the new optical device, developed and established at the Institut für Thermodynamik, Universität Hannover, Germany. All the gases investigated were obtained commercially, and were used without further purification. The suppliers and purity specification of our gas samples are given in Table I.

A. Measurement of $n(P,T)$ and determination of A_R

The absolute refractive index is obtained by counting the changes in the interference fringes while venting the gas under examination to vacuum. This reference to vacuum is necessary because interferometric measurements record only changes in the refractive index. Absolute refractive indices $n(P,T)$ are calculated from the interference fringe count by means of the data reduction formula,

$$n(P,T) = K(P,T)\lambda_0/l + 1, \quad (13)$$

where $K(P,T)$ is the total fringe count while isothermally venting the gaseous sample at pressure P to vacuum and l is the spacer length at the temperature T of the fluid.

TABLE I. Suppliers and minimum stated purity of the gases used.

Gas	Supplies	Stated minimum purity (%)	Nature of main impurities
CH_4	Messer–Griesheim	99.9995	$O_2 < 0.5$ ppm, $N_2 < 2$ ppm, $H_2O < 2$ ppm, $H_2 < 0.1$ ppm, $C_nH_m < 0.1$ ppm, $CO_2 < 0.1$ ppm
C_2H_4	Messer–Griesheim	99.95	$O_2 < 15$ ppm, $N_2 < 50$ ppm, $H_2O < 30$ ppm, $CH_4 < 200$ ppm, $C_2H_6 < 150$ ppm, $C_nH_m < 100$ ppm
C_2H_6	Messer–Griesheim	99.95	$O_2 < 10$ ppm, $N_2 < 40$ ppm, $H_2O < 5$ ppm, $CO_2 < 10$ ppm, $C_nH_m < 400$ ppm
CO_2	Messer–Griesheim	99.995	$O_2 < 25$ ppm, $N_2 < 25$ ppm, $CO < 1$ ppm, $C_nH_m < 1$ ppm
SF_6	Kali–Chemie	99.998	$N_2 < 2$ ppm, $H_2O < 1.2$ ppm
H_2	Messer–Griesheim	99.999	$O_2 < 1$ ppm, $N_2 < 5$ ppm, $H_2O < 5$ ppm, $C_nH_m < 0.1$ ppm, $CO/CO_2 < 0.1$ ppm
N_2	Messer–Griesheim	99.9995	$O_2 < 0.5$ ppm, $H_2O < 2$ ppm, $C_nH_m < 0.1$ ppm, $CO/CO_2 < 0.1$ ppm, Ar < 3 ppm
He	Linde	99.996	$O_2 < 5$ ppm, $N_2 < 20$ ppm, $H_2O < 5$ ppm, $C_nH_m < 1$ ppm, Ne < 10 ppm
Ar	Linde	99.998	$O_2 < 3$ ppm, $N_2 < 10$ ppm, $H_2O < 5$ ppm, $C_nH_m < 0.2$ ppm

The first refractivity virial coefficient A_R can be determined directly by means of an independent method in which only isothermal (P,n,T) measurements are involved. The density ρ in Eq. (1) can be replaced with the use of the thermodynamic virial equation of state

$$Z = P/\rho RT = 1 + B(T)\rho + C(T)\rho^2 + \cdots, \quad (14)$$

where $B(T)$, $C(T)$, ... are the virial coefficients of the compression factor Z, and R is the molar gas constant with the latest value[22] given by $R = (8.314\,471 \pm 0.000\,014)$ J/K mol. Dividing Eq. (1) by Eq. (14) and substituting ρ by the inverse function of $L_n = A_R\rho + B_R\rho^2 + C_R\rho^3 + \cdots$, given by $\rho = L_n/A_R - (L_n/A_R)^2 B_R/A_R + \cdots$, we obtain

$$RTL_n/P = A_R + [B_R - B(T)A_R]L_n/A_R + \cdots, \quad (15)$$

or, equivalently,

$$RTL_n/P = A_R + [B_R - B(T)A_R]P/RT + \cdots. \quad (16)$$

For convenience, the symbol L_n is used for the refraction $(n^2-1)/(n^2+2)$. When one plots experimental values of RTL_n/P vs L_n, Eq. (15) or RTL_n/P vs P, Eq. (16), one can determine A_R from the intercept with an accuracy of a few parts in 10^4.

The accuracy of A_R depends on the use of the coefficient to derive other parameters, such as B_R, C_R, ..., or $\rho(P,T)$. The uncertainty in the value of B_R or C_R is about two orders of magnitude higher than that of A_R and as such they are not affected by the uncertainty in the value of A_R. In the case of the determination of $\rho(P,T)$ from $n(P,T)$ the situation is quite different, because the uncertainty of A_R essentially determines the uncertainty of $\rho(P,T)$ in the lower density range. To obtain accurate values of $\rho(P,T)$ from $n(P,T)$ measurements, accurate values of A_R with an uncertainty of only few parts in 10^4 are required.[18]

For the accurate determination of A_R we used the extensive refractive index measurements $n(P,T)$ up to pressures of 35 MPa, which were carried out on the same gases at different isotherms to determine the density $\rho(P,T)$.[19,25]

Estimates of the first refractivity virial coefficient A_R were obtained from a least-squares fit of Eq. (15) to the $n(P,T)$ values. We used Eq. (15) instead of Eq. (16), because the slope at the point of inflection for the plot of RTL_n/P vs L_n is less steep than the corresponding slope for the plot of RTL_n/P vs P. As the precision of these measurements decreases rapidly at lower pressures, we also included measurements at higher pressures for the determination of A_R, but excluded experimental points which are in the vicinity and above the point of inflection of the curve RTL_n/P vs L_n. In Fig. 2, we plotted the experimental values of RTL_n/P

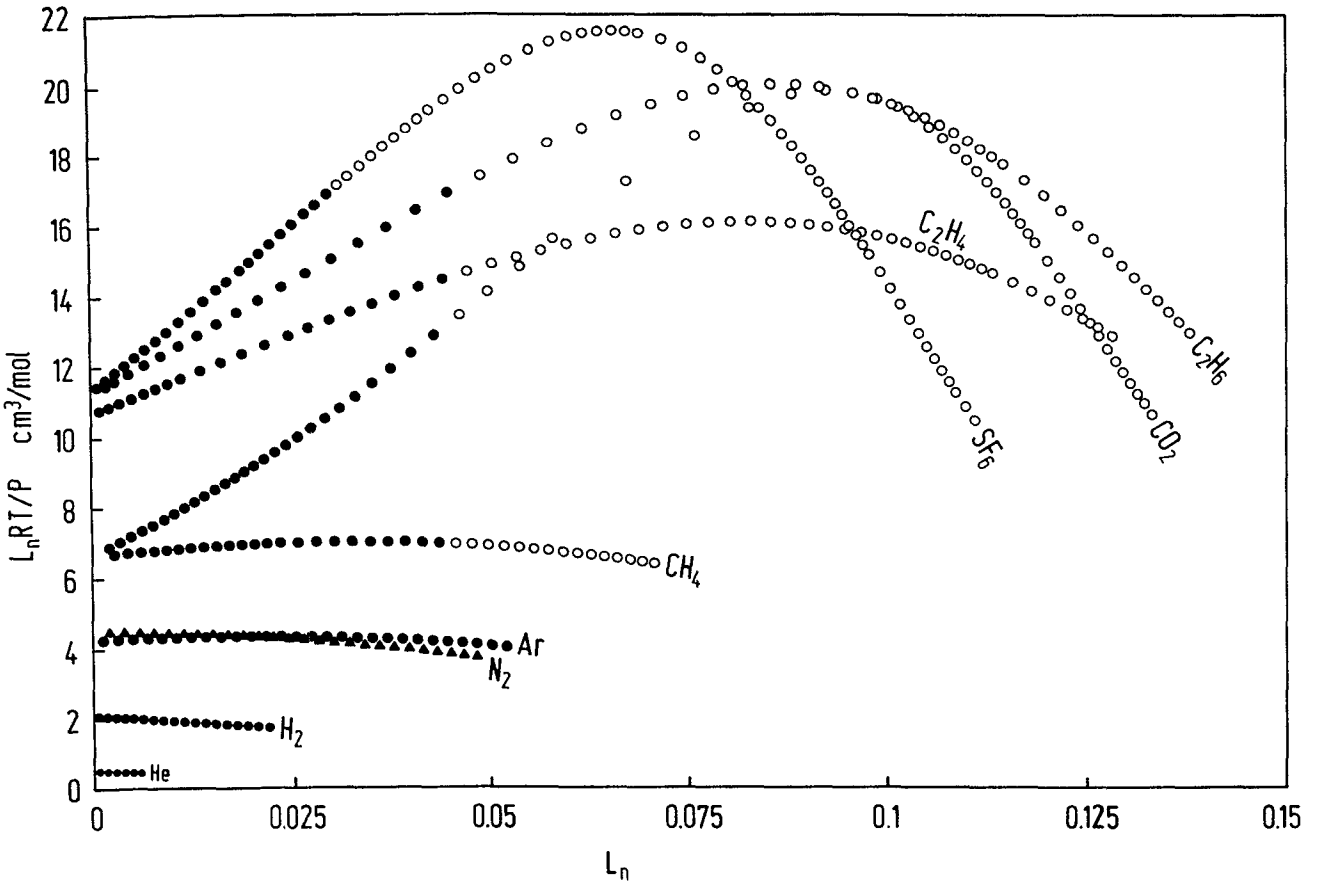

FIG. 2. Experimental values of $RT\ L_n/P$ for CO_2, H_2, N_2, He, and Ar at 323.15 K and for CH_4, C_2H_4, C_2H_6, and SF_6 at 373.15 K. The intercept gives A_R the zero density (or L_n) limit. The filled symbols indicate the experimental points which were used for the least-squares fit to determine A_R. To avoid the overlapping of experimental points, we plotted only a reduced number of measured values.

as a function of L_n for the nine gases investigated and indicated the values used for the least-squares fit as filled symbols, whereas the open circles are the disregarded values. To avoid the overlapping of experimental points we plotted only a reduced number of the values measured. For the purpose of comparison, our observed values of A_R with their uncertainty are summarized in Table II together with the experimental and computed literature values. The values of A_R, computed from data in Landolt–Börnstein Tables,[12,23] agree very well with our experimental values.

B. Measurements of $\Delta K(K,T)$ and determination of B_R, C_R, and D_R

The differential measurements were made for CH_4, CO_2, H_2, N_2, He, and Ar on the 323.15 K isotherm and for CH_4, C_2H_4, C_2H_6, and SF_6 on the 373.15 K isotherm and at pressures up to 35 MPa. The density range extends from 0.7 up to twice the critical density.

The contribution to the fringe count ΔK_{AB} and ΔK_{BA} arising from the distortion of cells and compensation chambers under pressure is rather significant. This effect not only depends on the geometry of the cells and compensation chambers but also on the type of sample gas used. Since in our case the volume of the cells (2 cm^3) is negligible compared to the volume of the compensation chambers (200 cm^3), only the cylindrical pipe of the compensation chamber with the external and internal radii R_e(7 mm) and R_i(4 mm) at a given initial pressure P_1 determine the systematic error in ΔK due to distortion. If we also take into account the real-gas behavior expressed by Z_1 and Z_2, the compression factor values before and after the expansion, the contribu-

TABLE II. Summary of the present experimental values for A_R, B_R, C_R, and D_R and literature values of A_R, B_R, and C_R. Calculated values of A_R have been computed from Landolt-Börnstein Tables (Ref. 23). Experimental values for the refractivity virial coefficients have been determined at the vacuum wavelength of $\lambda_0 = 632.99$ nm, except for the values of CH_4 from Olson (Ref. 9), ($\lambda = 546.2$ nm), C_2H_6 from Sliwinski (Ref. 10), ($\lambda = 589.3$ nm), H_2 from Diller (Ref. 8), ($\lambda = 546.2$ nm), the theoretical value for H_2 from Orcutt and Cole (Ref. 36), (λ infinite), and the values of He from Orcutt and Cole (Ref. 36) and Kirouac and Bose (Ref. 55), (λ infinite).

Gas	T (K)	A_R (cm^3/mol)	B_R (cm^6/mol^2)	C_R (cm^9/mol^3)	D_R (cm^{12}/mol^4)	Reference
CH_4	323	6.576 ± 0.002	6.08 ± 0.10	− 324 ± 5		This work
	373	6.576 ± 0.002	6.13 ± 0.15	− 317 ± 10		This work
	323	6.576 ± 0.002	5.83 ± 0.15	− 326 ± 10		Achtermann *et al.* (Ref. 25)
	298	6.578 ± 0.002	6.14 ± 0.20	− 345 ± 15		Montixi and Coulon (Ref. 26)
	220	6.613 ± 0.002	6.1 ± 1.0	− 320		Olson (Ref. 9)
	299	6.660	7.15 ± 0.35			Buckingham and Graham (Ref. 12)
	302	6.553 ± 0.002	6.60 ± 0.38			St-Arnaud and Bose (Ref. 13)
	···	6.569	7.76 ± 1.32			Burns *et al.* (Ref. 6)
	298	6.576	6.24			Theory (Ref. 12)
	302		6.11			Theory (Ref. 13)
	298		6.74			Theory (Ref. 6)
C_2H_4	373	10.656 ± 0.002	19.5 ± 0.5	− 1591 ± 84	5540 ± 2100	This work
	303	10.599 ± 0.009	17.6 ± 2.2			Bose *et al.* (Ref. 15)
	303	10.652 ± 0.002	17.7 ± 0.4	− 1280 ± 25		Achtermann and Beahr (Ref. 18)
	373	10.655 ± 0.002	17.8 ± 0.3	− 1280 ± 19		Achtermann and Baehr (Ref. 18)
	303	10.610 ± 0.009	40.8 ± 2.0			St-Arnaud and Bose (Ref. 27)
	303	10.649	21.8			Theory (Ref. 15)
C_2H_6	373	11.247 ± 0.003	26.6 ± 0.5	− 2227 ± 75	12 400 ± 3500	This work
	348	11.229 ± 0.006	22.9 ± 3.0	− 1560 ± 240		Jaeschke (Ref. 28)
	various	11.26 ± 0.02	27.8 ± 1.0	− 1990 ± 70		Sliwinski (Ref. 10)
	283		22.4			Theory (Ref. 10)
CO_2	323	6.644 ± 0.001	1.9 ± 0.2	− 287 ± 8		This work
	320	6.641 ± 0.003	0.0 ± 1.0	− 224 ± 40		Jaeschke (Ref. 28)
	299	6.650	3.2 ± 1.6			Buckingham and Graham (Ref. 12)
	298	6.590	4.75 ± 1.30			Burns *et al.* (Ref. 6)
	323	6.658 ± 0.021	3.3 ± 3.6			St-Arnaud and Bose (Ref. 14)
	298		4.38			Theory (Ref. 6)
	298		6.45			Theory (Ref. 12)
	···	6.647	6.9			Theory (Ref. 14)
SF_6	373	11.323 ± 0.002	22.7 ± 0.5	− 2783 ± 130	37 800 ± 8000	This work
	299	11.34	29 ± 5			Buckingham and Graham (Ref. 12)
	298	11.297	27.82 ± 5.18			Burns *et al.* (Ref. 6)
	323	11.348 ± 0.021	36.0 ± 1.8			St-Arnaud and Bose (Ref. 14)
	298		22.8			Theory (Ref. 6)
	···	11.410	24.8			Theory (Ref. 14)
	298		11.1			Theory (Ref. 12)
H_2	323	2.0713 ± 0.0001	0.13 ± 0.08	− 13.7 ± 2.0		This work
	298	2.0845 ± 0.0004				Diller (Ref. 8)

TABLE II. (*continued*).

Gas	T (K)	A_R (cm^3/mol)	B_R (cm^6/mol^2)	C_R (cm^9/mol^3)	D_R (cm^{12}/mol^4)	Reference
			0.036			Theory (Ref. 36)
N_2	323	4.4464 ± 0.0005	0.89 ± 0.06	-99.8 ± 2.8		This work
	323	4.446 ± 0.001	0.64 ± 0.08	-107 ± 5		Achtermann *et al.* (Ref. 25)
	299	4.460	1.0 ± 0.3			Buckingham and Graham (Ref. 12)
	298	4.446	0.74 ± 0.65			Burns *et al.* (Ref. 6)
	298	4.4454 ± 0.0005	0.75 ± 0.10	-85 ± 10		Montixi *et al.* (Ref. 7)
	298	4.458	1.50			Theory (Ref. 6)
	298		1.75			Theory (Ref. 7)
	298		1.89			Theory (Ref. 12)
He	323	0.5213 ± 0.0001	-0.068 ± 0.010			This work
	323	0.519 ± 0.001	-0.06 ± 0.04			Orcutt and Cole (Ref. 36)
	303	0.5210 ± 0.0002	-0.059 ± 0.009[a]	-0.84 ± 1.20		Kirouac and Bose (Ref. 55)
	294		-0.062			Theory (Ref. 59)
Ar	323	4.196 ± 0.0002	1.76 ± 0.05	-86.6 ± 2.0		This work
	298	4.1973 ± 0.0005	1.49 ± 0.15	-79 ± 10		Coulon *et al.* (Ref. 29)
	299	4.207	2.16 ± 0.34			Buckingham and Graham (Ref. 12)
	298	4.194	1.57 ± 0.58			Burns *et al.* (Ref. 6)
	303		2.0			Theory (Ref. 15)
	298		2.55			Theory (Ref. 6)
	298		2.04			Theory (Ref. 12)

[a]The uncertainty in the paper by Kirouac and Bose (Ref. 55) given as ± 0.0009 is changed to ± 0.009 because of a printing error in the earlier paper.

tion to the fringe count due to distortion of the compensation chamber to ΔK_{expt} is

$$\Delta K_{\Delta V} = RT\lambda_0 \Delta R_i K_1^2 (2Z_1 - Z_2)/lA_n P_1 R_i. \quad (17)$$

A similar expression for $\Delta K_{\Delta V}$ was developed by Buckingham and Graham[12] without the factor $(2Z_1 - Z_2)$. Buckingham and Graham[12] carried out the differential measurements only in the lower range of pressure up to approximately 0.5 MPa. In this range, the contribution of $(2Z_1 - Z_2)$ can be neglected, because its value goes to unity as the pressure decreases to zero. According to Landau and Lifshitz,[24] the apparatus constant of the compensation chamber $\Delta R_i/PR_i$ is given as

$$\Delta R_i/PR_i = [R_e^2(1+\sigma) + R_i^2(1+\sigma)(1-2\sigma)]/(R_e^2 - R_i^2)E, \quad (18)$$

where ΔR_i is the change in radius due to the pressure P, E is the Young's modulus (2×10^{11} Pa), and σ is the Poisson ratio (0.3).

The corrected value ΔK is given by

$$\Delta K = \Delta K_{\text{expt}} + \Delta K_{\Delta V}. \quad (19)$$

Since the form of the compensation chambers is nearly ideal (long pipes), the calculation of its distortion under pressure is very satisfactory. The effect of error correction, $\Delta K_{\Delta V}/\Delta K$, is largest at the highest pressure.

The significant values for B_n, C_n, and D_n can be obtained from the best least-squares fit of the error-corrected experimental values of the refractive index function F in a polynomial of the form

$$F = a_1 x + a_2 x^2 + a_3 x^3 + \cdots, \quad (20)$$

where $x = [(n_A - 1) + (n_B - 1)]$, $a_1 = B_n/2A_n^2$, $a_2 = (3A_nC_n - 4B_n^2)/8A_n^4$, and $a_3 = (20B_n^3 - 26A_nB_nC_n + 7A_n^2D_n)/32A_n^6$, etc.

We found that in the investigated range of $[(n_A - 1) + (n_B - 1)]$ the best least-squares fit of F for the gases CH_4, CO_2, Ar, H_2, and N_2 was given by a polynomial of the second degree, and for the gases C_2H_4, C_2H_6, and SF_6 by a polynomial of the third degree. Using the polynomial of the form $F = a_0 + a_1 x + \cdots$, we found that the intercept a_0 was practically zero within the experimental error for all gases investigated.

Our values for B_R, C_R, and D_R are summarized in Table II together with the literature values. The second refractivity virial coefficients B_R of H_2 and He, the third refractivity virial coefficients C_R of SF_6 and H_2,and the fourth refractivity virial coefficients D_R are given for the first time. The quoted uncertainties for B_R, C_R, and D_R are obtained by taking three standard deviations from the least-squares fit as well as errors due to cell distortion and adsorption.[18]

Contrary to all the other gases examined in this work, our measurements of $\Delta K(K,T)$ for He at 323.15 K and pressures up to 35.7 MPa give for the function $F(x,T)$ a straight-line relationship along the x axis. We measured $\Delta K(K,T)$ for He in the range 15.3–35.7 MPa,and repeated the experiments ten times at 35.7 MPa. The measured mean value of the fringe count at 35.7 MPa and 323.15 K yielded for He: $(\Delta K_{\text{expt},AB} + \Delta K_{\text{expt},BA})/2 = -0.58 \pm 0.10$, where for the absolute fringe count the value of $K = 1351$ was measured. At 35.7 MPa, the systematic error was calculated for $\Delta K_{\Delta V}$, Eq. (17), to be 0.56. For He using Eq. (19) and substituting

these values for ΔK_{expt} and $\Delta K_{\Delta V}$, the corrected value of the fringe count, ΔK, is practically zero. Consequently, each of the terms of the series F, Eq. (8), must also be zero within the experimental error. Therefore, the value of $B_R = -0.068\ \text{cm}^6/\text{mol}^2$ was only due to the contribution of the term $-A_n^2/9$, Eq. (4). If the correction of the systematic error $\Delta K_{\Delta V}$ in ΔK_{expt} is neglected, the value of B_R for He decreases from -0.068 to $-0.1\ \text{cm}^6/\text{mol}^2$.

In Fig. 3 we plotted the experimental values of F, the calculated function F from the least-squares fit and the calculated linear and quadratic terms of F for CO_2 at 323.15 K. The graph of a_2x^2 indicates from which value of $[(n_A - 1) + (n_B - 1)]$ or pressure the coefficient C_n becomes significant and exceeds the experimental error in F. In Fig. 4 we plotted the experimental values of F, the calculated function of F from the least-squares fit, and the calculated linear, quadratic, and cubic terms of F for SF_6 at 373.15 K. The graph of a_3x^3 indicates, as does a_2x^2 for C_n, at which value of $[(n_A - 1) + (n_B - 1)]$ or pressure the contribution of the D_n term of the function F becomes significant and exceeds the experimental error in F. The coefficients a_1, a_2, and a_3 were obtained from the least-squares fit, Eq. (20). In addition to the independent variable $[(n_A - 1) + (n_B - 1)]$, in the lower abscissa, we give corresponding values of pressures of 0.5, 5, 10, 15, 20, 25, 30, and 35 MPa in the upper abscissa in Figs. 3 and 4. The corresponding values of $[(n_A - 1) + (n_B - 1)]$ for the markings of the pressures were calculated from the measured relation $n(P,T)$. The pressure of 0.5 MPa is also given because Buckingham and Graham[12] and Burns *et al.*[6] carried out the overflow experiments up to this value of pressure.

In Fig. 5 we plotted the correlation functions F for the nine gases studied. The analysis of the refractive index function F shows that, for each gas examined, the B_n and C_n terms of F are always significant in the investigated range of pressure, except for He, where the B_n and C_n term is zero. The values of a_1 and a_2 for CH_4 at 323.15 and 373.15 K are the same within the experimental error. Therefore a significant temperature dependence of B_R and C_R was not found in the investigated range of temperature. The accurate determination of B_n and C_n requires an estimation of the D_n term, because neglecting a real D_n term leads to misfitting of the refractive index function F, and therefore to the determination of erroneous values of B_n and C_n. The method generally used to fit the data properly consists of fitting the data to successively higher-order polynomials, and the polynomial giving the lowest standard deviation is chosen.

We also determined the number of significant coefficients B_n, C_n, D_n, ... by graphical techniques based on interrelated plots of the residual quantities of the refractive index function $F = a_1x + a_2x^2 + a_3x^3 + \cdots$ in the relations

$$F/x = a_1 + a_2x + a_3x^2 + \cdots \tag{21}$$

and

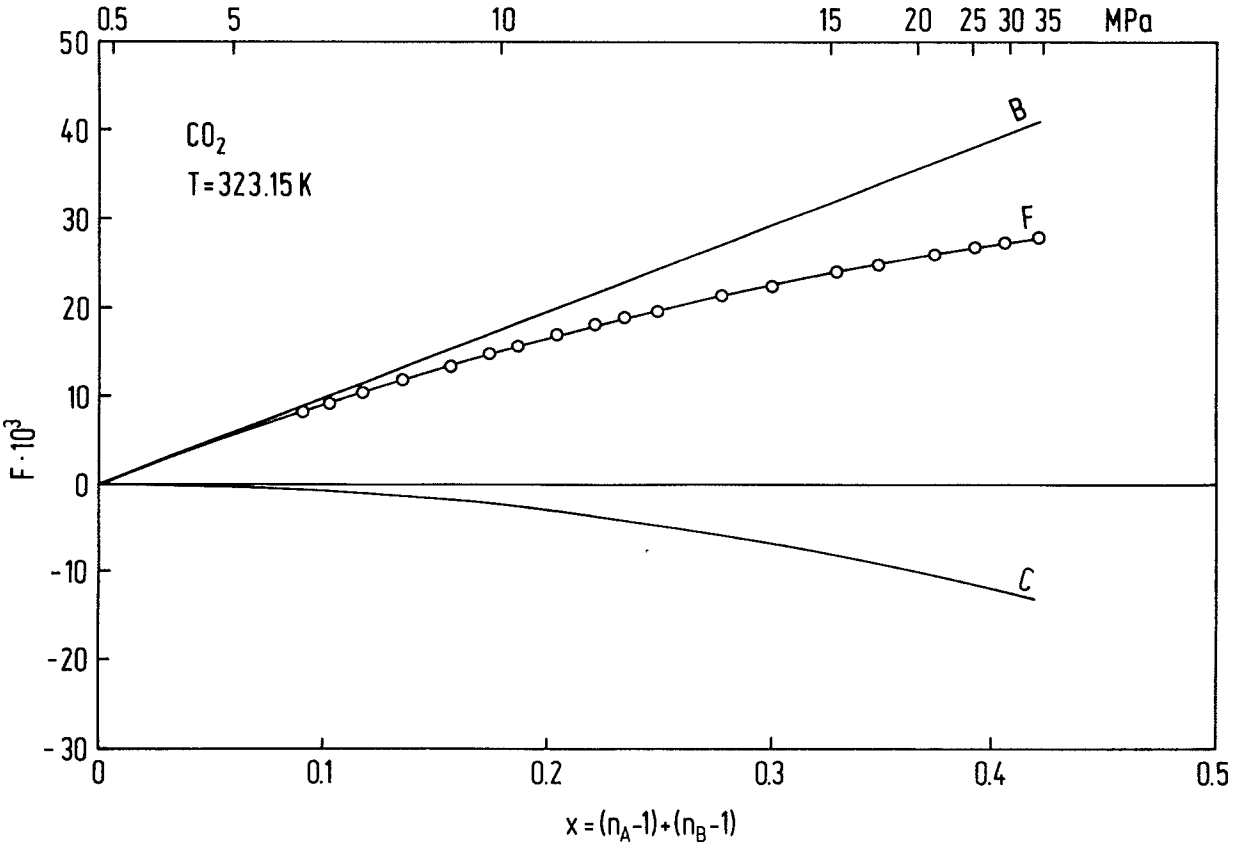

FIG. 3. Experimental values of the refractive index function F at 323.15 K for CO_2. The best least-squares fit of the experimental values of F as well as the linear and the quadratic terms of $F = a_1x + a_2x^2$ are also plotted. The symbols B and C are used to label the terms a_1x and a_2x^2. The figures at the upper margin are values of pressure which correspond to x. For convenience, the symbol x is used for the independent variables $[(n_A - 1) + (n_B - 1)]$.

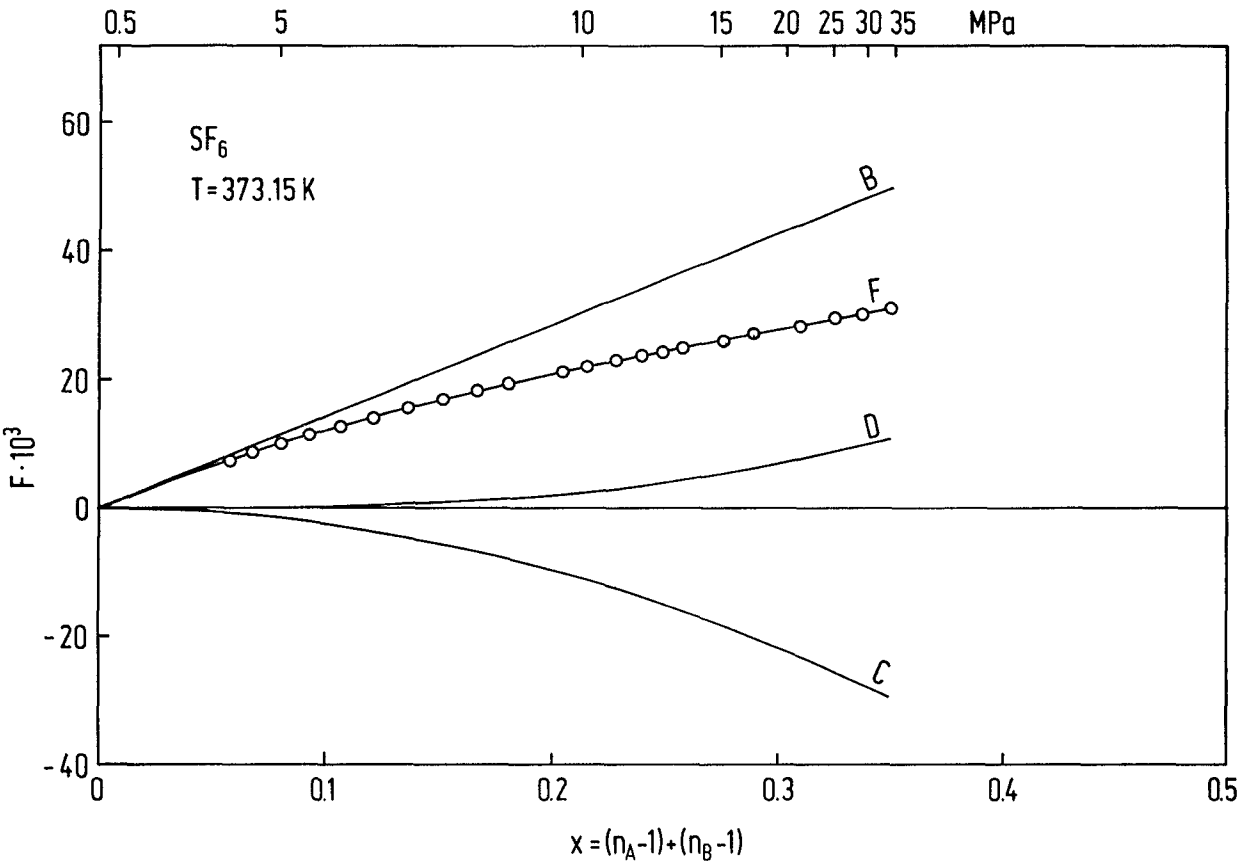

FIG. 4. Experimental values of the refractive index function F at 373.15 K for SF_6. The best least-squares fit of the experimental values of F as well as the linear, quadratic, and cubic term of $F = a_1x + a_2x^2 + a_3x^3$ are also plotted. The symbols B, C, and D are used to label the terms a_1x, a_2x^2, and a_3x^3. The figures at the upper margin are values of pressure which correspond to x. For convenience, the symbol x is used for the independent variable $[(n_A - 1) + (n_B - 1)]$.

$$(F/x - a_1)/x = a_2 + a_3x + \cdots . \tag{22}$$

To determine the significant coefficients a_1, a_2, a_3,..., we plotted successive experimental values of F,F/x, and $(F/x - a_1)/x$ vs x. The intercept as well as the slope of the functions are unique to only one of the coefficients in the above relations, whereas the curvature can be influenced by more than one coefficient. In the graph F vs x, the B_n term determines the slope and all the succeeding terms of B_n cause the curvature of F. In the graph F/x vs x, the B_n term determines the intercept, the C_n term the slope, and all the succeeding terms of C_n cause the curvature of F/x. No evidence of curvature in F/x indicates that the contribution of the D_n term is negligible in the investigated range of x. If the experimental results show any evidence of curvature, we also plot $(F/x - a_1)/x$ vs x, where the C_n term determines the intercept and the D_n term the slope. Because the D_n term contributes significantly to the above functions only at higher values of x, we give precedence to examining the experimental values in this region,whether or not the points can be fitted by a straight line.

The experimental points of the investigated gases CH_4, CO_2, H_2, N_2, and Ar show a straight-line plot in the graph F/x vs x, whereas for C_2H_4, C_2H_6, and SF_6 the straight-line plot of the experimental points first appears in the graph $(F/x - a_1)/x$ vs x. Figure 6 shows the results of SF_6 and CO_2 as examples of the nine gases investigated. The values of SF_6 indicate obvious curvature in the F/x graph, whereas the results of CO_2 indicate no evidence of curvature even at higher values of x. Figures 7(a) and 7(b) show the results of SF_6 and CO_2 in the graph $(F/x - a_1)/x$ vs x. The constant slope of the SF_6 plot indicates that terms higher than D_n are not significant in the investigated range of x and the plot of CO_2 again shows that the D_n term is not significant in the investigated range of x. Graphs F/x and $(F/x - a_1)/x$ are also more sensitive to the scattering of the experimental points than the plot of F. Since the scatter of the measurements at low pressures increases rapidly, we always started with the measurements in the high pressure region. We also used the F/x and $(F/x - a_1)/x$ plots to determine the low-pressure range in which it is not useful to continue the overflow experiments because the experimental values scatter too much and do not contribute to the accuracy of B_n, C_n,... .

In Fig. 8 we plotted the relative excess contribution $(R_m - A_R)/R_m$ as a function of density for the gases investigated, except for He. The functions were calculated by means of the measured significant refractivity virial coefficients, given in Table II. It is seen that the functions $(R_m - A_R)/R_m$ initially increase with density to a maxi-

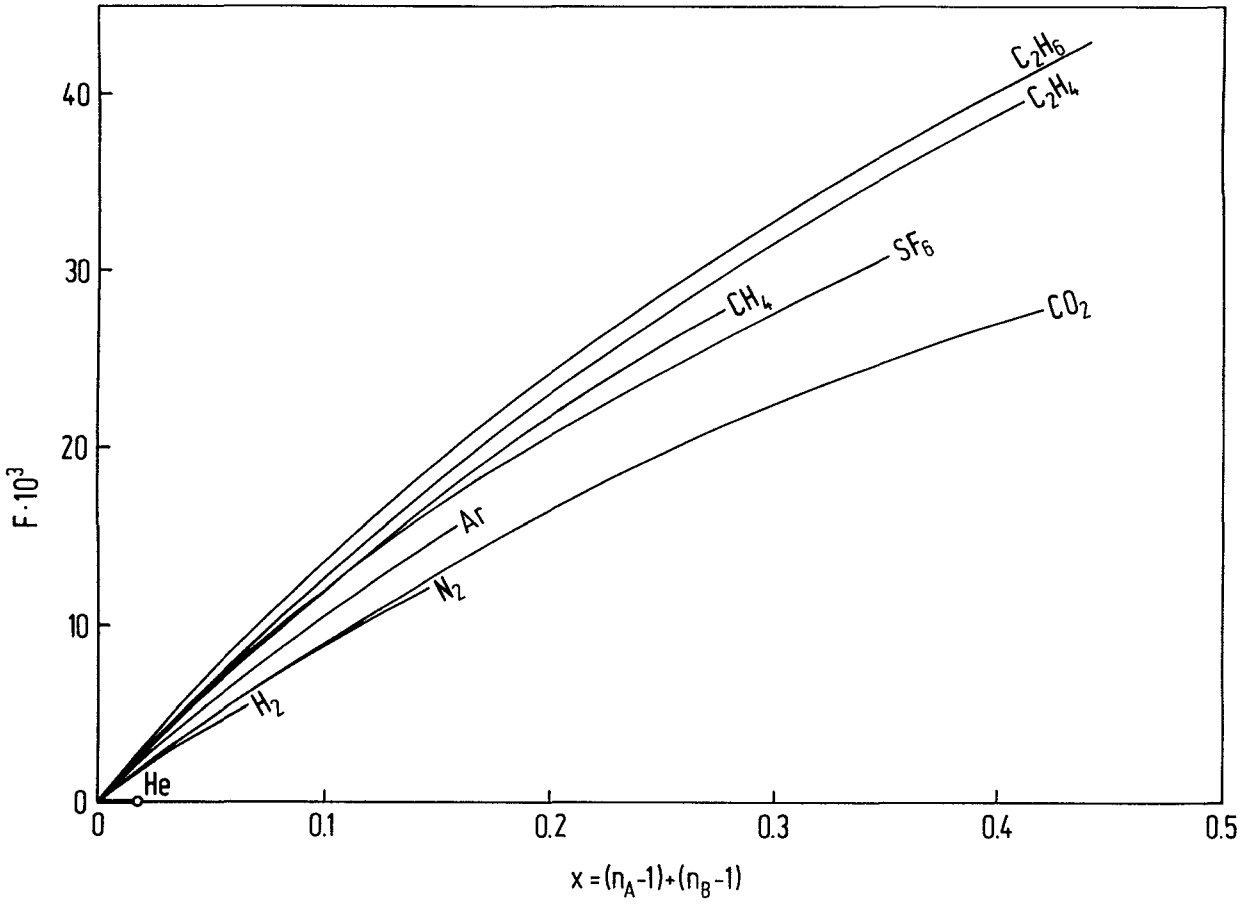

FIG. 5. Refractive index functions F for the nine gases investigated. The curves represent the experimental values and are calculated with the coefficients a_1,a_2, and a_3 from the least-squares fit. For convenience, the symbol x is used for the independent variable $[(n_A - 1) + (n_B - 1)]$.

mum, and then decrease with increasing density. The lower limit of the maximum amplitude of $(R_m - A_R)/R_m$ is reached by H_2 at 0.015% and the higher limit of the maximum is attained by C_2H_6 at 0.73%. The functions of $(R_m - A_R)/R_m$ for CO_2, SF_6, H_2, and N_2 decrease in the investigated density range to values below the low-density limit. This behavior is in qualitative agreement with theoretical models[31,36,37] and other experimental results of R_m of nonpolar fluids.[3-5,7-10,29] It is also very similar to the experimental values of the Clausius–Mossotti relation, *CM*, for nonpolar fluids.[39,40] For the R_m and *CM* functions the theoretical calculations predict a slight increase with density to the critical density, and then a decrease at higher densities. The filled circle on each function marks the point where the density is equal to the critical density. We extrapolated $(R_m - A_R)/R_m$ to higher values of density, because the critical density for Ar, H_2, and N_2 lies outside the range of our measurements. The position of the maximum of $(R_m - A_R)/R_m$ for CH_4, C_2H_4, C_2H_6, SF_6, and Ar is in qualitative agreement with the theory, in the vicinity of the critical density, whereas for CO_2, H_2, and N_2 the maximum already appear at densities that are approximately half the value of the critical density. The sharp decrease of $(R_m - A_R)/R_m$ for CO_2 was also observed by Michels and Hamers.[41]

IV. DISCUSSION

In this section we compare our results of B_R and C_R with other experimental and theoretical values. Buckingham and Graham[12] and Burns *et al.*[6] have already investigated the gases CH_4, CO_2, SF_6, N_2, and Ar, but they carried out the differential measurements only in the small range of pressure of approximately 0.5 MPa. The contribution of the C_n term in F is practically nonexistent in this very small range of pressure. Even for SF_6 the contribution of the C_n term is only about 1% of F at 0.5 MPa, and therefore within its experimental error, see Fig. 4. Nevertheless, if we consider the small range of pressure examined, the agreement between the experimental values of B_R published by Buckingham and Graham[12] and Burns *et al.*[6] and our B_R values is quite good, see Table II. St-Arnaud and Bose[13,27,14] measured differentially the refractive index function F for CH_4, C_2H_4, CO_2, and SF_6 and Bose *et al.*[15] for C_2H_4 and C_2H_4–Ar mixtures. All the measurements were carried out using a Michelson laser interferometer (model HP-5501 A) operating at the vacuum wavelength of 632.99 nm. St-Arnaud and Bose[13] measured the refractive index function F for CH_4 in the pressure range 12–18 MPa. Their B_R value of (6.60 $\pm$ 0.38) cm^6/mol^2 agrees with our B_R value of (6.08 $\pm$ 0.10) cm^6/mol^2 within the experimental error. They,

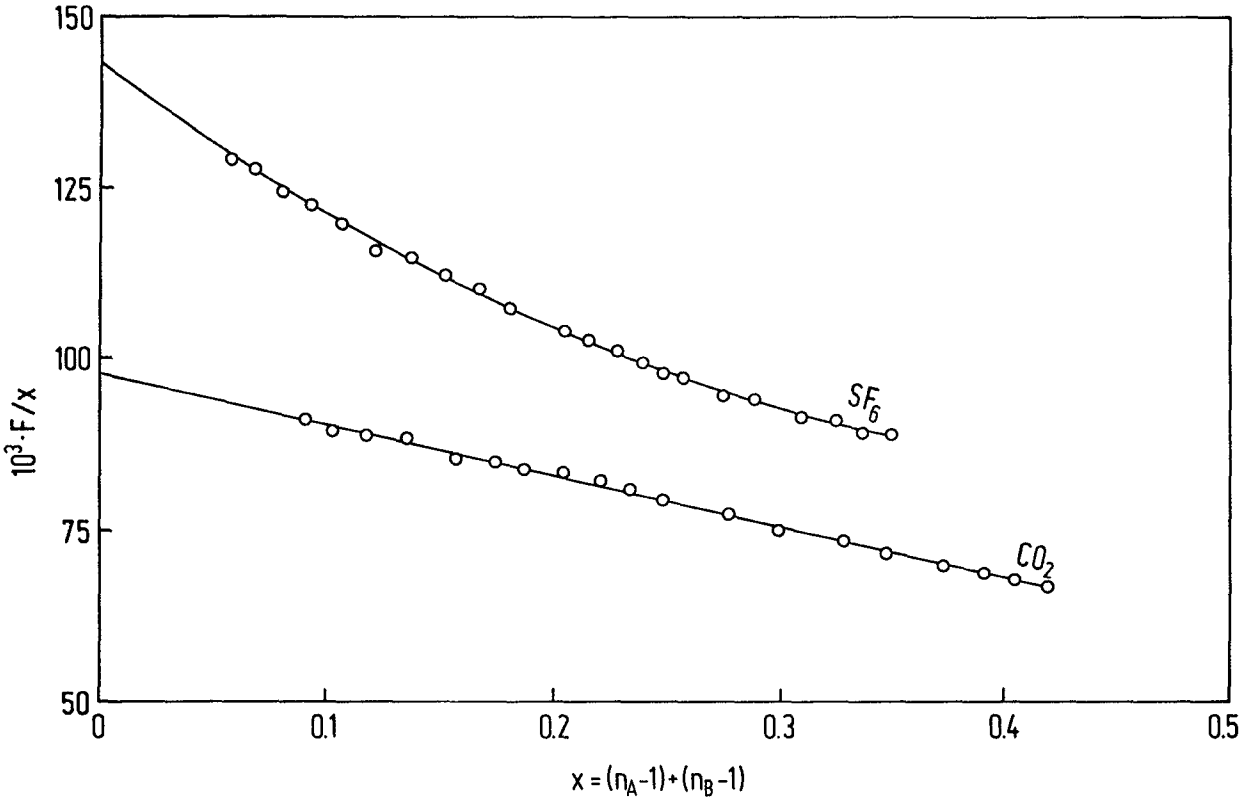

FIG. 6. Plots of F/x for CO_2 at 323.15 K and SF_6 at 373.15 K. For convenience, the symbol x is used for the independent variable $[(n_A - 1) + (n_B - 1)]$. Points are experimental and the curves are the least-squares fit.

however, give no value of C_R. At 12 MPa and 323.15 K our results show a contribution of the C_n term of 11% and at 18 MPa of 15%. Neglecting a significant C_n term causes a reduction of the value of B_R. If we used our experimental values of F in the pressure range up to 10 MPa and neglect the C_n term, we then obtain a reduced value of B_R of 4.7 cm^6/mol^2 compared to B_R of 6.08 cm^6/mol^2 by including the C_n term (see also Ref. 11). In the case of C_2H_4 the experimental B_R value of Bose *et al.*[15] agrees within the experimental error with our B_R value. Again, no C_R value is given for this gas. The B_R value of CO_2 measured by St-Arnaud and Bose[14] agrees within the experimental error with our B_R value. Their high pressure measurements of F for CO_2 differ considerably from our results. St-Arnaud and Bose[14] measured F of SF_6 to pressures of approximately 4 MPa and deduced a B_R value of (36.0 ± 1.8) cm^6/mol^2. This value considerably exceeds our experimental B_R of (22.7 ± 0.5) cm^6/mol^2. Determination of C_R is not possible from their measurements of F in this range of pressure, because the contribution of the C_n term to F is within the experimental error. The difference we observe between the high pressure measurements of F of St-Arnaud and Bose[13,27,14] and Bose *et al.*[15] and our own, may be due to the fact that the differential measurement carried out by them in the high pressure region was not a direct measurement of the fringe count during the expansion of the sample. Considerable error creeps into the experimental result if ΔK_{AB} or ΔK_{BA} is measured as a difference between two large numbers. The experimental values of B_R and C_R for CH_4 and N_2 by Achtermann *et al.*,[25] obtained by using the same apparatus as in this work, deviate slightly from present experimental values, because in the previous paper the systematic error in F due to the distortion of cells and compensation chambers under pressure was not corrected. Achtermann and Baehr[18] gave values of B_R and C_R for C_2H_4 by taking account of some of the corrections but not the contribution of the factor $(2Z_1 - Z_2)$ as shown in Eq. (17).

We shall now compare our experimental values of B_R and C_R with other results obtained by the absolute method. Our values of B_R and C_R for CH_4 agree well with the results of Montixi and Coulon[26] and Olson.[9] Montixi and Coulon[26] as well as Olson[9] determined B_R and C_R by combining $n(P,T)$ with $\rho(P,T)$ values to pressures of about 20 MPa. The density sets used are from different sources. The experimental values of B_R and C_R for C_2H_6 by Sliwinski[10] agree remarkably well with our values if one considers that Sliwinski[10] combined $n(P,T)$ with $\rho(P,T)$ values only up to densities of 0.005 88 mol/cm^3, whereas our densities reach 0.013 mol/cm^3. Jaeschke[28] determined B_R and C_R for C_2H_6 and CO_2 by a fit of $\rho(P,T)$ values from the optical PVT method to Burnett data. The values of B_R are somewhat smaller than our values, and the C_R values somewhat greater than our C_R, see Table II. Diller[8] measured R_m of hydrogen, but values of the higher-order refractivity virial coefficients of H_2 are not given. The B_R value of H_2 of 0.13 cm^6/mol^2 is very small, because $2B_n/3$ is nearly equal to $A_n^2/9$, Eq. (4).

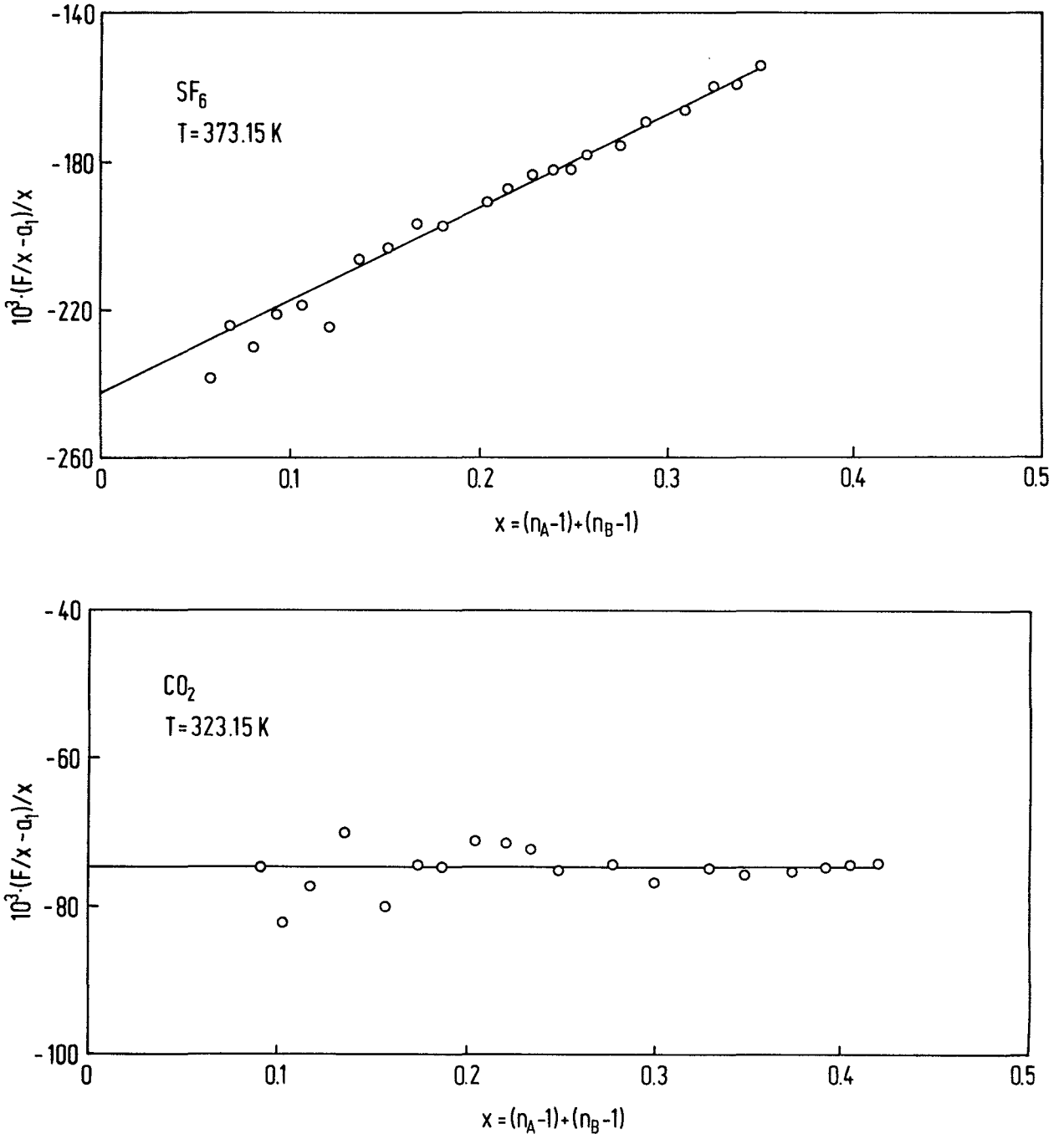

FIG. 7. (a), (b) Plots $(F/x - a_1)/x$ for CO_2 at 323.15 K and SF_6 at 373.15 K. For convenience, the symbol x is used for the independent variable $[(n_A - 1) + (n_B - 1)]$. Points are experimental and the curves are the least-squares fit.

Montixi *et al.*[7] determined B_R and C_R for N_2 by combining $n(P,T)$ with $\rho(P,T)$ values in the pressure range 4–40 MPa. The agreement between the values obtained by Montixi *et al.*[7] and our experimental values of B_R and C_R is quite good. To the best of our knowledge, B_R of He has never been measured before. The negative value of B_R that we determine is corroborated by the negative B_ϵ value observed by using differential dielectric constant measurements by Orcutt and Cole[36] and Kirouac and Bose[55] and absolute dielectric constant measurements at low temperatures (2.6 to 27.1 K) by Gugan and Michel[56] and Gugan.[57] From the experimental results of the fringe count, we estimated the range of the C_R value. If we assign the whole experimental error of the fringe count as well as errors due to cell distortion and adsorption to the C_n term, we obtain the range of C_n and from this the range of C_R as $-1.0\ \text{cm}^9/\text{mol}^3 < C_R < 0.4\ \text{cm}^9/\text{mol}^3$. Kirouac and Bose[55] gave for He a C_ϵ value of $(-0.84 \pm 1.20)\ \text{cm}^9/\text{mol}^3$. As He is an atomic gas, the dielectric virial coefficients A_ϵ, B_ϵ, and C_ϵ should be equal to the refractivity virial coefficients A_R, B_R, and C_R (see Table

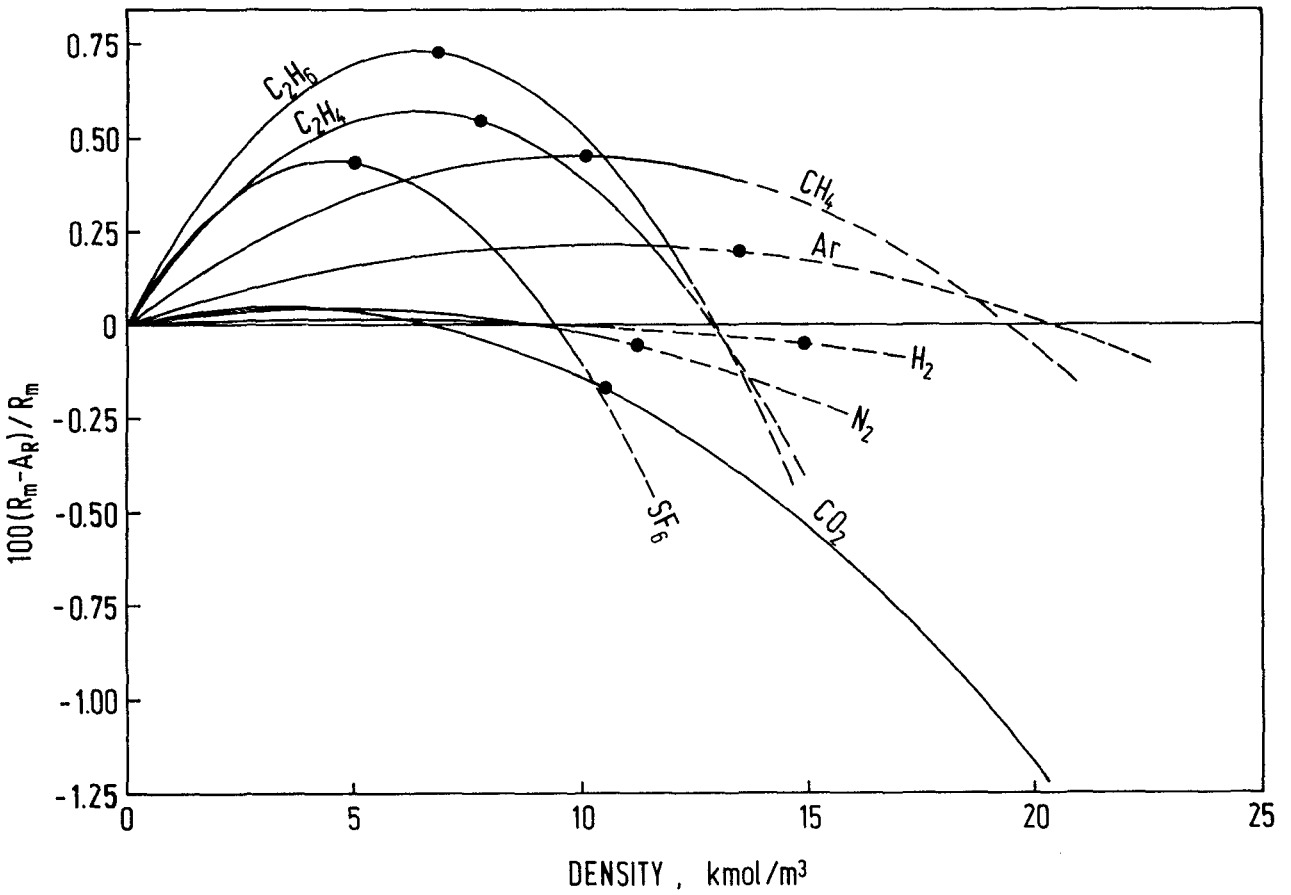

FIG. 8. Relative excess contribution $10^2(R_m - A_R)/R_m$ of the gases investigated, except for He. The filled circles mark the points where the density is equal to the critical density. The dashed lines denote the extrapolated part of the functions.

II), depending on the refractive index measurement being outside the frequency range of the dispersion region. Our experimental values of B_R and C_R for Ar agree rather well with the experimental values of Coulon *et al.*[29]

Although in general we obtained good agreement between our results for B_R and C_R using the differential method with those obtained by the absolute method, the later suffers from the fact that high accurate values of $\rho(P,T)$ are needed up to approximately two times the critical density for an unambiguous determination of B_R and C_R. It should, however, also be mentioned that in the case of the absolute method, the use of $B(T)$, Eq. (15), instead of the whole $\rho(P,T)$ surface, could lead to large errors in the determination of B_R.[14]

We shall now compare our experimental B_R with the theoretical values. The analytical expression for B_R is given by the classical statistical-mechanical equation[1]

$$B_R = (N_A^2/3\epsilon_0\Omega)\int[(1/2)\alpha_{12}(\tau) - \alpha_0] \times \exp[-U_{12}(\tau)/kT]\,d\tau, \qquad (23)$$

where $\alpha_{12}(\tau)$ is the mean polarizability of a molecule when participating in a binary collision, α_0 the polarizability of an isolated molecule, and $U_{12}(\tau)$ the potential energy of the pair 1,2 in the relative configuration τ, and Ω is the integral over angular coordinates defined by $\Omega\rho = \int d\tau$. Using a point dipole approximation, the incremental polarizability $\Delta\alpha(r) = [1/2\alpha_{12}(\tau) - \alpha_0]$ may be calculated by the so-called dipole induced dipole (DID) model. The incremental polarizability is then given by $\Delta\alpha(r) = 2(\alpha_0^3/r^6)$.[58] It is clear that the above expression of $\Delta\alpha(r)$ always gives a positive B_R. This contradicts the experimental fact that at room temperature B_R is negative for He and Ne. Even though the experimental values of B_R for Ar, N_2, etc. are positive, the agreement with the DID theory is not satisfactory. The reason for this discrepancy is that the DID model neglects the effect of both the long-range and short-range interactions on molecular polarizability. The quantum mechanical calculation of the long-range effect on the polarizability is positive. This increases the discrepancy even more between the calculated and the experimental values of B_R. Thus, in order to have a realistic calculation, the short-range effect must be taken into account. As far as theory is concerned, a complete calculation including both the long-range and short-range effects on the polarizability have been carried out only for the lightest gases like He and Ne. Therefore the comparison of our experimental B_R values with the theoretical calculation has to be limited to classical DID model except for He and Ne where detailed calculations have been carried out by Dacre.[59]

For the quasispherical molecule CH_4 Burns *et al.*[6] rep-

resented the potential energy by the Lennard-Jones (L-J) (6–12) potential. The calculation was made with the L-J parameters derived from viscosity measurements in preference to that obtained from the virial coefficient because the viscosity technique is more sensitive to the symmetric part of the potential. Among the B_R values calculated by Burns *et al.*[6] using different pairs of reported ϵ/k and R_0, the best agreement between theory and our experiment is given with $B_R = 6.74$ cm^6/mol^2, calculated with the reported values[30] of $\epsilon/k = 137.0$ K and $R_0 = 0.388$ nm. St-Arnaud and Bose[13] calculated B_R of CH_4 with L-J viscosity parameters of $\epsilon/k = 148.6$ K and $R_0 = 0.3758$ nm. The given B_R of 6.11 cm^6/mol^2 agrees extremely well with our experimental B_R of 6.08 cm^6/mol^2.

For C_2H_4 the only theoretical calculation that exists for B_R is the value of Bose *et al.*[15] based on the DID model. Our experimental B_R of 19.5 cm^6/mol^2 agrees well with the calculated B_R of 21.8 cm^6/mol^2 using viscosity derived L-J parameters[30] $\epsilon/k = 230$ K and $R_0 = 0.4066$ nm.

For C_2H_6 Sliwinski[10] calculated a classical theoretical B_R value of 22.4 cm^6/mol^2 using the viscosity derived L-J parameters[30] $\epsilon/k = 230$ K and $R_0 = 0.4418$ nm. This value agrees rather well with our experimental B_R of 26.6 cm^6/mol^2.

For CO_2 St-Arnaud and Bose[14] calculated a classical theoretical B_R value of 6.9 cm^6/mol^2 with the Lennard-Jones(6–12) potential and the L-J parameters $\epsilon/k = 218.8$ K and $R_0 = 0.3819$ nm. This value is in disagreement with our experimental B_R of 1.9 cm^6/mol^2. One can, however, understand the discrepancy if one notes that the point dipole approximation (DID model) neglects the effect of both long-range and short-range interactions on molecular polarizability. Although Burns *et al.*[6] included four contributions to calculate the difference $[(1/2)\alpha_{12}(\tau) - \alpha_0]$ for CO_2, the total calculated B_R of 4.38 cm^6/mol^2 is still in disagreement with our B_R. The smaller calculated value of Burns *et al.*[6] is caused by a significant negative contribution to B_R from a term proportional to α^2/R^3.

St-Arnaud and Bose[14] calculated a classical theoretical B_R for SF_6 based on a generalized Lennard-Jones (7–28) potential[32] and the L-J parameters of $\epsilon/k = 439$ K and $R_0 = 0.468$ nm. Our experimental B_R of 22.7 cm^6/mol^2 agrees reasonably well with the classically calculated value of 24.8 cm^6/mol^2. Buckingham and Clarke Hunt[33] also reported on an improved agreement between experiment and theory with the use of a modified Lennard-Jones (7–28) potential. Burns *et al.*[6] calculated theoretical values for B_R with the Lennard-Jones (6–12) potential and also with a modified Lennard-Jones (7–28) potential with the L-J parameters $\epsilon/k = 414$ K and $R_0 = 0.503$ nm. The Kirkwood[38] fluctuation term (DID model) rises from 16.39 cm^6/mol^2 calculated with the L-J(6–12) potential to 18.72 cm^6/mol^2 obtained with the modified Lennard-Jones(7–28) potential. Burns *et al.*[6] reported that the contribution of the C term to B_R, which describes the excess field at molecule 1 due to a quadrupole induced on 2 by the field gradient of a dipole induced on 1 by the external field, could not be calculated owing to the lack of data for SF_6. An estimated C-term contribution of 20% yields a B_R of 22.8 cm^6/mol^2, which is within the experimental limits of the measured B_R of 27.28 cm^6/mol^2 by Burns *et al.*[6] whereas this value agrees extremely well with our experimental B_R of 22.7 cm^6/mol^2.

For H_2 there exists no theoretical calculation for B_R. The calculated theoretical value of B_ϵ by Orcutt and Cole[36] should be similar to B_R (see Table II).

The classical calculation of B_R without consideration of the shape factor for the rod-like molecules N_2 yields values of B_R which exceed considerably our observed value of 0.89 cm^6/mol^2. Buckingham and Graham[12] calculated a B_R of 1.89 cm^6/mol^2 and Montixi *et al.*[7] a B_R of 1.75 cm^6/mol^2. A shape factor of 0.2 for CO_2 was determined by Datta and Sing[42] in their calculation of multipole moments from viscosity and second virial coefficients. There is no reported shape factor for N_2, and for their calculations Burns *et al.*[6] used an arbitrarily chosen shape factor of 0.2 according to the above constraint for rod-like molecules. The calculated B_R of 1.50 cm^6/mol^2 still exceeds the observed value. If the shape factor for N_2 is assigned the value 0.4 (the shape factor for rod-like molecules lies between 0 and 0.5) the corresponding calculated B_R of 0.71 cm^6/mol^2 is then smaller than our experimental value.

Dacre[59] calculated for He a theoretical value of the second dielectric virial coefficient using the various *ab initio* trace values together with the so-called HFDHE2 potential developed by Aziz *et al.*[60] The potential is relatively simple but realistic in form and more accurate than the Hartree–Fock potential which would overemphasize the repulsion, since electron correlation, which is incorporated in the best potentials, will lower the total energy and hence the repulsion. It was fitted to accurate intermediate temperature second virial coefficients and thermal conductivity data as well as high temperature viscosity values. Dacre[59] calculated at 294 K the total SCF + CI trace and found B_ϵ (SCF + CI) $= -0.062$ cm^6/mol^2. This is very close to the accurate experimental B_ϵ value of Kirouac and Bose[55] of (-0.059 ± 0.009) cm^6/mol^2 at 303 K and of the experimental B_R of this work (-0.068 ± 0.010) cm^6/mol^2 at 323 K.

The calculated B_R of 2.55 cm^6/mol^2 for Ar by Burns *et al.*,[6] with the L-J viscosity parameters $\epsilon/k = 124.0$ K and $R_0 = 0.3418$ nm is considerably larger than our experimental B_R of 1.76 cm^6/mol^2. Bose *et al.*[15] calculated with the L-J viscosity parameters[30] $\epsilon/k = 124$ K and $R_0 = 0.3418$ nm a B_R of 2.0 cm^6/mol^2, which is slightly larger than our experimental B_R. The greater theoretical B_R, calculated with the DID model, is in conformity with what one finds in the case of all atomic gases and in the case of CO_2.[34,35]

In Table III, we compare the relationship that exists between the dielectric and the refractivity virial coefficients on the one hand and the collision induced absorption on the other. For a gas one can always express the dielectric constant ϵ like the refractive index n in the form of a virial expansion

$$CM = (\epsilon - 1)/(\epsilon + 2)\rho = A_\epsilon + B_\epsilon\rho + C_\epsilon\rho^2 + \cdots, \tag{24}$$

where A_ϵ, B_ϵ, C_ϵ, ... are, respectively, the first, second,

TABLE III. Comparison of B_{OR} ($= B_\epsilon - B_R$) with the sum of $B_{FIR} + B_{IR}$.

Gas	T (K)	B_ϵ expt (cm^6/mol^2)	B_R expt (cm^6/mol^2)	B_{OR} (cm^6/mol^2)	B_{FIR} expt (cm^6/mol^2)	B_{IR} calc (cm^6/mol^2)	$B_{FIR} + B_{IR}$ (cm^6/mol^2)
CO_2	296	60.0[a]	1.9[c]	58.1	62 ± 6 (Ref. 43)	1.0 (Ref. 44)	63
	302.6	57.6 ± 0.9 (Ref. 34)					
	322.9	50.7 ± 0.9 (Ref. 34)	1.9 ± 0.2[b]	48.8 ± 0.9			
CH_4	279.8	8.14 ± 0.29 (Ref. 45)					
	303	7.7[a]	6.11[c]	1.6	1.66 (Ref. 51)	0.087 (Ref. 44)	1.75
	322.5	7.29 ± 0.32 (Ref. 45)					
	323.15		6.11 ± 0.10[b]				
	373.4	6.75 ± 0.29 (Ref. 45)	6.13 ± 0.15[b]	0.62 ± 0.30			
C_2H_4	298	50.3[a]	19.5[c]	30.8	32.5 ± 2.8 (Ref. 52)	0.8 (Ref. 15)	33.3
	323.1	47.5 ± 1.4 (Ref. 46)					
	373.1	42.0 ± 2.8 (Ref. 46)	19.5 ± 0.5[b]	22.5 ± 2.8			
	423.1	37.6 ± 2.4 (Ref. 46)					
SF_6	298	65.6[a]	22.7[c]	42.9	0.53 (Ref. 50)	24.2 (Ref. 44)	24.7
	323.3	63.31 ± 2.80(Ref. 49)					
	348.3	60.54 ± 1.45 (Ref. 49)					
	373.9	58.84 ± 4.70 (Ref. 49)	22.7 ± 0.5[b]	36.14 ± 4.73			
N_2	323.1	2.1 ± 0.1 (Ref. 48)	0.89 ± 0.06[b]	1.2 ± 0.1	1.26[d] (Ref. 47)		

[a] Extrapolated values.
[b] This work.
[c] Estimated, based on the temperature independence of B_R values within the small range of temperature.
[d] Computed from the experimental values of α_1 and γ_1 given by Stone *et al.* (Ref. 47) by using the approximate relation $\int \omega^{-2}\alpha(\omega)d\omega = \gamma_1 - (1/3)(h/2kT)^2\alpha_1$ to obtain the Kramers–Kronig integral.

third, ... dielectric virial coefficients. For a multipolar gas, the dielectric second virial coefficient will include two terms:

$$B_\epsilon = B_{OR} + B_{IND}, \tag{25}$$

where B_{OR} measures the contribution of the pair interaction of the induced dipole moments produced by the multipolar field (molecular field) and B_{IND} is the contribution of the pair interaction of the induced dipole moments produced by the applied external field. B_R corresponds to B_{IND} because B_{OR}, being of molecular origin, does not contribute at optical frequencies.

It is also possible to determine the virial coefficients associated with a given band denoted by the subscript λ from measurements of the absorption coefficient $\alpha_\lambda(\omega)$.[43] Thus by using the Kramers–Kronig relation

$$(\epsilon - n^2)_\lambda = \frac{2c}{\pi}\int_0^\infty \omega^{-2}\alpha_\lambda(\omega)d\omega \tag{26}$$

and the virial expansion

$$\int_0^\infty \omega^{-2}\alpha_\lambda(\omega)d\omega = A_\lambda\rho + B_\lambda\rho^2 + C_\lambda\rho^3 + \cdots, \tag{27}$$

where c is the velocity of light and ω is the angular frequency. We obtain

$$A_{IR} = \frac{2c}{\pi}\sum_\lambda A_\lambda, \tag{28}$$

$$B_{FIR} = \frac{2c}{\pi}\sum_\lambda B_\lambda, \tag{29}$$

where to sufficient approximation, we use $\epsilon + 2 = n^2 + 2 = 3$. The sum in Eq. (28) is taken over all rotation–vibration (R–V) bands in the infrared (IR) region which vary as ρ. If the molecules possess no permanent dipole moment, the case of interest here, $A_{IR} = A_\epsilon - A_R$ is due only to infrared vibrational transitions and is very much smaller than A_ϵ and A_R.[53] The sum in Eq. (29) is taken over all translation–rotation (T–R) microwave and far infrared (FIR) band varying as ρ^2. The quantity B_{IR} is also given by Eq. (29), where the sum is over all translation–rotation–vibration (T–R–V) bands in the infrared region varying as ρ^2.

It is clear from Table III, that a comparison between B_{OR}, derived from our newly measured B_R values and literature values of B_ϵ, on the one hand and $B_{FIR} + B_{IR}$ on the other for different multipolar gases is rather good for most systems except for SF_6. In fact, SF_6 is still poorly understood. The recent work on SF_6 by Chapados and Birnbaum[54] fails to solve the problem as far as large unknown collision induced absorption bands are concerned. Although the collision induced absorptions are small in the case of CH_4 and N_2, we still have an excellent agreement between B_{OR} and $B_{FIR} + B_{IR}$. This type of agreement indeed shows to what extent the precision measurements for B_ϵ and B_R are now possible. Such precision equilibrium measurements for the dielectric and refractivity virial coefficients indeed put them in the same level as collision induced absorption in the far infrared as far as integrated values are concerned for the determination of multipole moments.

V. CONCLUSIONS

We have made highly accurate and precise measurements of the refractive index function F and refractive index measurements $n(P,T)$, up to pressures of 35 MPa. The overflow experiments to determine F were extended to high values of pressure. Compared with earlier measurements the fringe count was always carried out during the actual expansion, thus increasing the accuracy of the measurements. On

the other hand, errors due to distortion grow with increasing pressures. Significant positive contributions to the observed fringe count due to distortion have to be taken into account even with cells and compensation chambers having extremely thick walls. For gases like C_2H_4, C_2H_6, CO_2, and SF_6, where the value of the compressibility factor Z_1 approaches 0.2, the factor $(2Z_1 - Z_2)$, Eq. (17), is essential for the complete correction of the systematic error due to distortion. We have therefore corrected the effects of distortion in all the measured refractive index functions F of the gases investigated by means of Eq. (17), which is a modified form of the relation by Buckingham and Graham.[12] Our values of A_R, B_R, C_R, and D_R were also used to calculate the density $\rho(P,T)$ from measurements of the refractive index $n(P,T)$ in the pressure range investigated (up to 35 MPa). The good agreement of $\rho(P,T)$ with accurate values from other sources is a good consistency test of the accuracy of the refractivity virial coefficients. PVT isotherms are particularly sensitive to A_R in the lower density region, whereas for higher densities the influence of terms involving $B_R, C_R, \ldots$ increases. This kind of consistency test gives us confidence in the reliability of the various refractivity virial coefficients given in this paper.

ACKNOWLEDGMENTS

The authors H. J. A. and G. M. are grateful to the Deutsche Forschungsgemeinschaft for financial support of this work. We would like to thank T. Biermann, D. Hauser, K. Huhnholz, H. J. Neitzel, and W. Steingass for valuable assistance in computer calculation and technical help.

[1] A. D. Buckingham, Trans. Faraday Soc. **52**, 747 (1956).
[2] A. D. Buckingham, R. H. Cole, and H. Sutter, J. Chem. Phys. **52**, 5690 (1970).
[3] A. Michels, H. Lebesque, L. Lebesque, and S. R. deGroot, Physica **13**, 337 (1947).
[4] A. Michels, A. Botzen, and S. R. deGroot, Physica **13**, 343 (1947).
[5] A. Michels and A. Botzen, Physica **15**, 769 (1949).
[6] R. C. Burns, C. Graham, and A. R. M. Weller, Mol. Phys. **59**, 41 (1986).
[7] G. Montixi, R. Coulon, and R. Occelli, Can. J. Phys. **61**, 473 (1983).
[8] D. E. Diller, J. Chem. Phys. **49**, 3096 (1968).
[9] J. D. Olsen, J. Chem. Phys. **63**, 474 (1975).
[10] P. Sliwinski, Z. Phys. Chem. **63**, 263 (1969).
[11] H. J. Achtermann and H. Rögener, *Proceedings of the 8th Symposium on Thermophysical Properties* (ASME 1, 142, 1982).
[12] A. D. Buckingham and C. Graham, Proc. R. Soc. A **336**, 275 (1974).
[13] J. M. St-Arnaud and T. K. Bose, J. Chem. Phys. **65**, 4854 (1976).
[14] J. M. St-Arnaud and T. K. Bose, J. Chem. Phys. **71**, 4951 (1979).
[15] T. K. Bose, K. Boudjarane, J. Huot, and J. M. St-Arnaud, J. Chem. Phys. **89**, 7435 (1988).
[16] H. J. Achtermann, G. Magnus, and R. Scharf, VDI Forschungsh. **619** (1983).
[17] T. K. Bose, J. M. St-Arnaud, H. J. Achtermann, and R. Scharf, Rev. Sci. Instrum. **57**, 26 (1986).
[18] H. J. Achtermann and H. D. Baehr, VDI Forschungsh. **649** (1988).
[19] H. J. Achtermann, H. D. Baehr, and T. K. Bose, J. Chem. Thermodyn. **21**, 1023 (1989).
[20] W. M. Gelbart, Adv. Chem. Phys. **26**, 106 (1974).
[21] H. J. Achtermann and H. Rögener, Tech. Messen **49**, 87 (1982).
[22] M. R. Moldover, J. P. M. Trusler, T. J. Edwards, J. B. Mehl, and R. S. Davis, J. Res. Natl. Bur. Stand. (U.S.) **93**, 85 (1988).
[23] Landolt-Börnstein, *Zahlenwerte und Funktionen* (Springer, Berlin, 1962), Band II, Teil 8.
[24] L. D. Landau and E. M. Lifshitz, *Theory of Elasticity* (Pergamon, London, 1959).
[25] H. J. Achtermann, T. K. Bose, M. Jaeschke, and J. M. St-Arnaud, Int. J. Thermophys. **7**, 357 (1986).
[26] G. Montixi and R. Coulon, C. R. Acad. Sci. t. **296**, 135 (1983).
[27] J. M. St-Arnaud and T. K. Bose, J. Chem. Phys. **68**, 2129 (1978).
[28] M. Jaeschke, *Gas Quality*, edited by G. J. van Rossum (Elsevier, Amsterdam, 1986).
[29] R. Coulon, G. Montixi, and R. Occelli, Can. J. Phys. **59**, 1555 (1981).
[30] J. O. Hirschfelder, C. F. Curtiss, and R. B. Bird, *Molecular Theory of Gases and Liquids* (Wiley, New York, 1967).
[31] A. D. Buckingham and J. A. Pople, Trans. Faraday Soc. **51**, 1029 (1955).
[32] J. C. McCoubrey and N. M. Singh, Trans. Faraday Soc. **53**, 877 (1957).
[33] A. D. Buckingham and K. L. Clarke Hunt, Mol. Phys. **40**, 643 (1980).
[34] T. K. Bose and R. H. Cole, J. Chem. Phys. **52**, 140 (1970).
[35] A. D. Buckingham, R. L. Disch, and D. A. Dunmur, J. Am. Chem. Soc. **90**, 3104 (1968).
[36] R. H. Orcutt and R. H. Cole, J. Chem. Phys. **46**, 697 (1967).
[37] G. Stell and G. S. Rushbrooke, Chem. Phys. Lett. **24**, 531 (1974).
[38] J. G. Kirkwood, J. Chem. Phys. **4**, 592 (1936).
[39] J. F. Ely, H. J. M. Hanley, and G. C. Straty, J. Chem. Phys. **59**, 842 (1973).
[40] J. F. Ely and G. C. Straty, J. Chem. Phys. **61**, 1480 (1974).
[41] A. Michels and J. Hamers, Physica **4**, 995 (1937).
[42] K. K. Datta and Y. Sing, J. Chem. Phys. **55**, 3541 (1971).
[43] W. Ho, G. Birnbaum, and A. Rosenberg, J. Chem. Phys. **55**, 1028 (1971).
[44] G. Birnbaum and T. K. Bose, J. Chem. Phys. **71**, 17 (1979).
[45] T. K. Bose, J. Sochanski, and R. H. Cole, J. Chem. Phys. **57**, 3592 (1972).
[46] T. K. Bose and R. H. Cole, J. Chem. Phys. **54**, 3829 (1971).
[47] N. W. B. Stone, L. A. A. Read, A. Anderson, I. R. Dagg, and W. Smith, Can. J. Phys. **62**, 338 (1984).
[48] J. Huot and T. K. Bose (unpublished).
[49] C. Hosticka and T. K. Bose, J. Chem. Phys. **60**, 1318 (1974).
[50] A. Rosenberg and G. Birnbaum, J. Chem. Phys. **52**, 683 (1970).
[51] G. Birnbaum and E. R. Cohen, J. Chem. Phys. **62**, 3807 (1975).
[52] I. R. Dagg, L. A. A. Read, and W. Smith, Can. J. Phys. **60**, 1431 (1982).
[53] A. A. Maryott and F. Buckley, Natl. Bur. Stand. (U.S.) Circ. 537 (1953).
[54] C. Chapados and G. Birnbaum, J. Mol. Spectrosc. **132**, 323 (1988).
[55] S. Kirouac and T. K. Bose, J. Chem. Phys. **64**, 1580 (1976).
[56] D. Gugan and G. W. Michel, Metrologia **16**, 149 (1980).
[57] D. Gugan, Metrologia **19**, 147 (1984).
[58] A. D. Buckingham, P. H. Martin, and R. S. Watts, Chem. Phys. Lett. **21**, 186 (1973).
[59] P. D. Dacre, Mol. Phys. **45**, 17 (1982).
[60] R. A. Aziz, V. P. S. Nain, J. S. Carley, W. L. Taylor, and G. T. McConville, J. Chem. Phys. **70**, 4330 (1979).